Journal of Hazardous Materials 507 (2026) 141754

Contents lists available at ScienceDirect

Journal of Hazardous Materials

journal homepage: www.elsevier.com/locate/jhazmat

Radon transport in porous materials; application to the restoration of a phosphogypsum repository

E. Castaño-Casco *, I. Gutiérrez-Álvarez, A. Barba-Lobo, J.P. Bolívar

Radiation Physics and Environment Group (FRYMA), Centre for Natural Resources, Health and Environment (RENSMA), University of Huelva, Huelva 21007, Spain

HIGHLIGHTS

- An algorithm to calculate the radon exhalation of porous soils was developed.
- It was validated by literature comparison with models and measurements.
- An in-depth sensitivity analysis of the algorithm was done.
- The application to a phosphogypsum repository was in concordance with measurements.

GRAPHICAL ABSTRACT

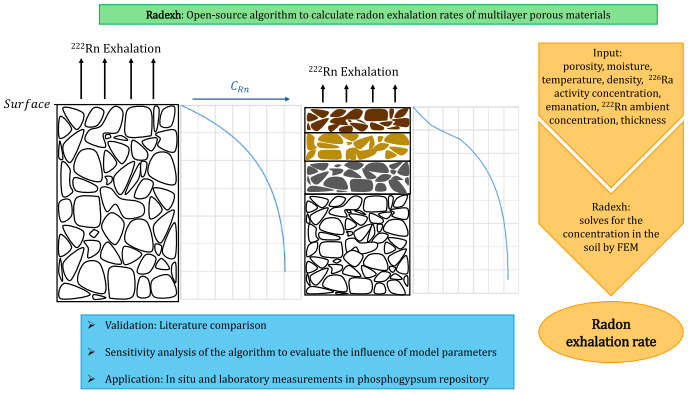

ARTICLE INFO

Keywords:
Radon
Radon exhalation
Phosphogypsum
Radon transport

ABSTRACT

The pilling of waste materials with high ^{226}Ra concentrations like phosphogypsum represents a potential health risk in many countries, making it important to understand radon transport through soils and develop mitigation techniques. The objective of this work is to develop and validate an open-source algorithm for evaluating radon transport through porous materials, and its application to estimate the radon exhalation depending on the applied restoration. Methodology has been validated by comparing our algorithm with literature data. A mean relative difference of 10% between our algorithm and the literature experimental measurements, and 14% with the literature model results were found. A sensitivity analysis was done by varying the input parameters and different boundary conditions were tested. The algorithm was compared against laboratory simulations of a phosphogypsum repository in Spain, with a mean relative difference of 13% compared with our results. Among the radon mitigation covers tested, the lowest exhalation was achieved by a geomembrane sheet. It was also tested with in-situ measurements of already restored sections of the repository finding a mean relative difference of 6% between the measurements and the algorithm. The measured topsoil cover reduction was 18%, and the algorithm estimated a 17% reduction in radon exhalation. In conclusion, an open-source alternative to the exhalation prediction of multi-layer soils was created, validated and gave accurate estimations.

* Corresponding author.
E-mail address: elena.castano@dci.uhu.es (E. Castaño-Casco).

https://doi.org/10.1016/j.jhazmat.2026.141754
Received 5 November 2025; Received in revised form 2 February 2026; Accepted 11 March 2026
Available online 13 March 2026

1. Introduction

The ^{238}U series radionuclides are among the most significant contributors to the radioactivity of the Earth's crust. In its decay chain, we find ^{226}Ra is found, which in turn decays to ^{222}Rn. ^{222}Rn ambient concentrations greatly depend on the local sources, which can be natural, or human made. In Huelva (Southern Spain) there is a phosphogypsum (PG) repository, a material that is a by-product from the production of phosphoric acid, used as fertiliser, which is created through the chemical treatment of phosphate rocks (PR). For every gram of PR processed, around 1.5 g of PG are produced [1–3]. PG is categorized as Naturally Occurring Radioactive Material (NORM) as phosphate rocks contain high levels of ^{238}U (about 50 times of ^{238}U in relation to unperturbed soils), and in relation to the radioactivity amount contained in PR, more than 95% of ^{226}Ra remains bound to the PG material [4–6].

Huelva factories processed from 1965 to 2010 about 2 million tons of PR annually, yielding 2.5–3 million tons of PG. Until 1998, the 20% of the PG produced was released to the Odiel River and the remaining 80% was stored in large piles, covering about 1000 ha of land near the factories on the right bank of the Tinto River channel. From 1998 onwards, the totality of the PG was stored in piles. The average concentration of ^{226}Ra in the PG stored in these stacks typically ranges from 500 to 1000 Bq kg^{-1}, with an average of 650 Bq kg^{-1}, which is 20 times higher than the background values found in typical soils [7–9]. Today there are 4 different zones. Zone 1 is a restored area with a soil cover of about 30 cm above the PG surface along with a vegetal cover. Zones 2 (up to 20 m height), and 3 are unrestored areas, while zone 4 is an already restored area. The presence of ^{226}Ra in PG will result in the release of ^{222}Rn gas, which is a health risk for workers and local populations. Waste management strategies include piling PG to increase its height rather than its surface area, which can reduce radon exhalation rates, and covering PG with different materials to minimize radon passing through [10–12]. In the Huelva repository the exhalation of different zones has been measured [8,9], finding the following ranges: 22–1220 Bq m^{-2} h^{-1} (zone 1), 800–7090 Bq m^{-2} h^{-1} (zone 2), and 110–1800 m^{-2} h^{-1} (zone 3). For zone 4 there are no published measurements before or after restoration. Values of radon exhalation from others PG repositories from around the world cover a wide range of values, varying between 200 – 18000 Bq m^{-2} h^{-1} [13–16]. The typical soil average value for exhalation is of 58 Bq m^{-2} h^{-1} [17,18], which is consistent with the values measured in an agriculture soil 75 km from the Huelva PG repository, ranging from 10 to 40 Bq m^{-2} h^{-1} [9].

The understanding of radon transport through a material is of great importance when studying and developing a possible solution to mitigate the risk of radon exposure caused by it [19–21]. The main terms in the transport equation are radon generation and decay, as well as diffusion and advection mechanisms, although most models generalize to a diffusion model when defining the problem equations [22,23]. The boundary conditions commonly used are of fix constant concentration value, ambient concentration, or null concentration at the top of the material, and the concentration at an infinite depth at the bottom of the material. Once the material concentration is known, calculating the resulting exhalation can help predict the final radon concentration to which the public is exposed.

Several researchers have developed a way to obtain the resulting radon exhalation from soil. In the stationary state, an analytical solution can be applied, as done by Zhuo et al. [24] and Wu et al. [25] in their one-dimensional diffusion model. In Zhuo et al. [24] they use a reformulated exhalation model with equations for the radon emanation factor and the radon diffusion coefficient depending on temperature, porosity and moisture content. To validate their results, they compare with experimental data obtained in their laboratory, which simulate the same conditions as the model input. In Wu et al. [25] the analytical solution was used to fit laboratory experimental data on radon concentration at different depths, to determine the radon diffusion coefficient of the soil and then the exhalation. The analytical solution is easier to apply, but less accurate. Another common approach is to use the finite element method (FEM) [10,26,27] or finite differences method (FDM) [28] to obtain a numerical solution. López-Coto et al. [10] uses a three-dimensional diffusion model in the transient state and solves for the divergence to the steady state using the Elmer tool. They also use an equation dependent of porosity and moisture for the diffusion

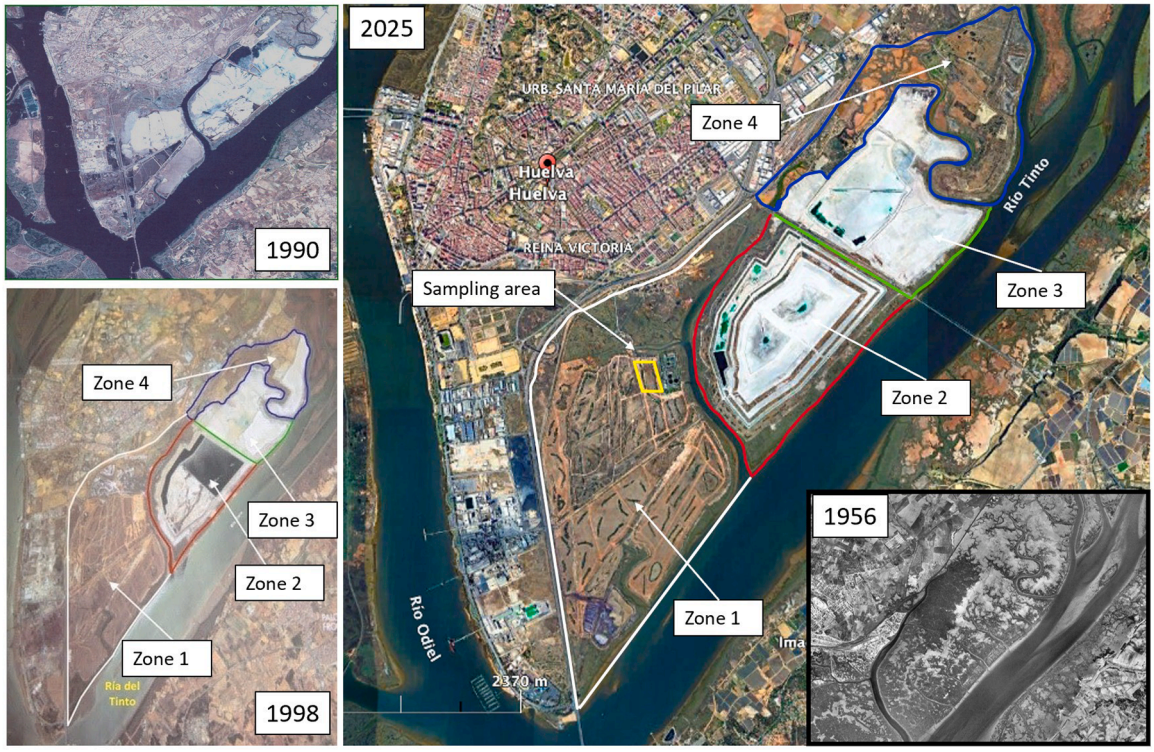

Fig. 1. Repository piles in the Huelva region at different times and sampling area location.

coefficient, studying the changes in the exhalation with these two parameters. Muñoz et al. [26] and Neznal et al. [27] both applied a two-dimensional stationary diffusion and advection model. [26] used COMSOL Multiphysics software and Neznal et al. [27] uses the special software RADON2D computer model to solve the numerical equation. Muñoz et al. [26] applies an equation dependent on porosity, moisture and temperature to calculate the radon diffusion coefficient, permeability and emanation rate. There are also one-dimensional stationary models with numerical solutions, such as Chitra et al. [28] They used a MATLAB finite difference scheme to solve a transient diffusion and advection model for the divergence to the steady state. In their work, they found that including advection only slightly altered the concentration profile under typical soil conditions.

The objective of this study was to develop and validate an open-source algorithm, RADEXH, that evaluates radon transport through contaminated material and a potential cover layer to calculate the final radon exhalation into the atmosphere. It was also investigated how changes in soil characteristics affect the radon exhalation rate and different boundary conditions for the problem were evaluated. As we cannot test the algorithm with in-situ or laboratory experiments involving a wide range of input parameters it was necessary to test the stability of the algorithm in these situations using a sensitivity analysis. Finally, the developed algorithm was applied, under real conditions, to the Huelva phosphogypsum repository case, comparing it with a laboratory simulation and in-situ measurements. It was important to compare not only with the controlled laboratory conditions, but also with real in situ conditions, in order to put the algorithm to the test. Fig. 1 shows a photo of the repository piles in the Huelva region, their evolution over time, and the location where the measurements for this study were taken.

The main novelty of this study is the easy access and application of a tool that will enable the study of the possible restauration of waste repositories and the estimation of the reduction in radon exhalation prior to its implementation. As the issue of PG pilling and its potential health risk is present in many countries, the impact of this study is not only relevant to the Huelva case study but also has global significance. There are many different tools for the solving transport equations, with the main novelty of RADEXH being its easy application, as it is specific to the problem of radon transport in waste material piles and the calculation of the radon exhalation rate. The model is a simplified version of the actual contaminant transport problem, reducing it to a one-dimensional stationary state. Its key benefit is that it is ready to use directly on multilayer contaminated porous soils, eliminating the need to learn and apply a FEM or similar tool to a specific problem. This makes predicting waste accumulation and possible restorations accessible to a wider range of people through an open-source program. The program will be made available via a GitHub repository.

2. Theory and algorithm

2.1. Theoretical framework

Certain assumptions have been made in the radon transport equation used; 1) transport is only considered in one dimension, along the x-axis, from the bottom to the surface of the material, as we assume homogeneity and linear transport; 2) the main mechanism for transport is assumed to be the diffusion, as the advection mechanism is only relevant in cases where the pressure gradient is significant such as high winds or entry into homes; and 3) we assume a steady state and no time dependence. The final radon transport equation is the following [29]:

$$D\frac{\mathrm{d}^2C(x)}{\mathrm{d}x^2} - \lambda_{Rn}C(x) + f = 0, \text{for} 0 \le x \le d \tag{1}$$

- $C(x)$: radon concentration in the porous space of the material (Bqm^{-3})
- x: position along the thickness of the material from the bottom to the surface (m)
- D: radon effective diffusion coefficient $(m^2\ s^{-1})$
- λ_{Rn}: radon decay constant (s^{-1})
- f: source term for the generation of radon from the material $(Bqm^{-3}\ s^{-1})$
- d: thickness of the material (m)

$$f = \lambda_{Rn}C_\infty = \lambda_{Rn}\frac{\rho C_{Ra}^{226}\varepsilon}{\beta} \tag{2}$$

- C_∞: maximal radon concentration in material pore space at large depth (Bqm^{-3})
- ρ: bulk density of the material (kgm^{-3})
- C_{Ra}^{226}: activity concentration of ^{226}Ra $(Bq\ kg^{-1})$
- ε: radon emanation
- β: effective porosity

$$\beta = (1 - s + sL)p \tag{3}$$

- p: porosity
- s: fraction of moisture saturation [30]
- L: Ostwald coefficient dependent on the temperature [31]

$$s = \frac{w\rho}{\rho_w p} \tag{4}$$

- w: water mass content [32]
- ρ_w: water density (kgm^{-3})

$$w = \frac{m_{wet} - m_{dry}}{m_{dry}} \tag{5}$$

- m_{wet}: wet mass in material (kg)
- m_{dry}: dry mass in material (kg)

$$RH = \frac{m_{wet} - m_{dry}}{m_{wet}} \tag{6}$$

- RH: relative humidity
- m_{dry}: dry mass in material (kg)

For the radon emanation rate an equation dependant on the moisture content can be used [33]:

$$\varepsilon = \varepsilon_0\left[1 + 1.8\left(1 - e^{-18.8s}\right)\right] \tag{7}$$

- ε_0: radon emanation in dry conditions

For the boundary conditions the literature usually uses ambient concentration for the surface of the material and the maximal concentration at the bottom [22,25,26], as we show in Eqs. 8–9.

$$C(x = 0) = C_\infty \tag{8}$$

$$C(x = d) = C_{amb} \tag{9}$$

- C_{amb}: radon ambient concentration (Bqm^{-3})

In this work, the condition used at the bottom of the soil was of zero radon flux (Eq. 10), as the condition for a fixed concentration is not appropriate for all soil thickness, being an approximation for large depths. The difference between both conditions will be demonstrated in

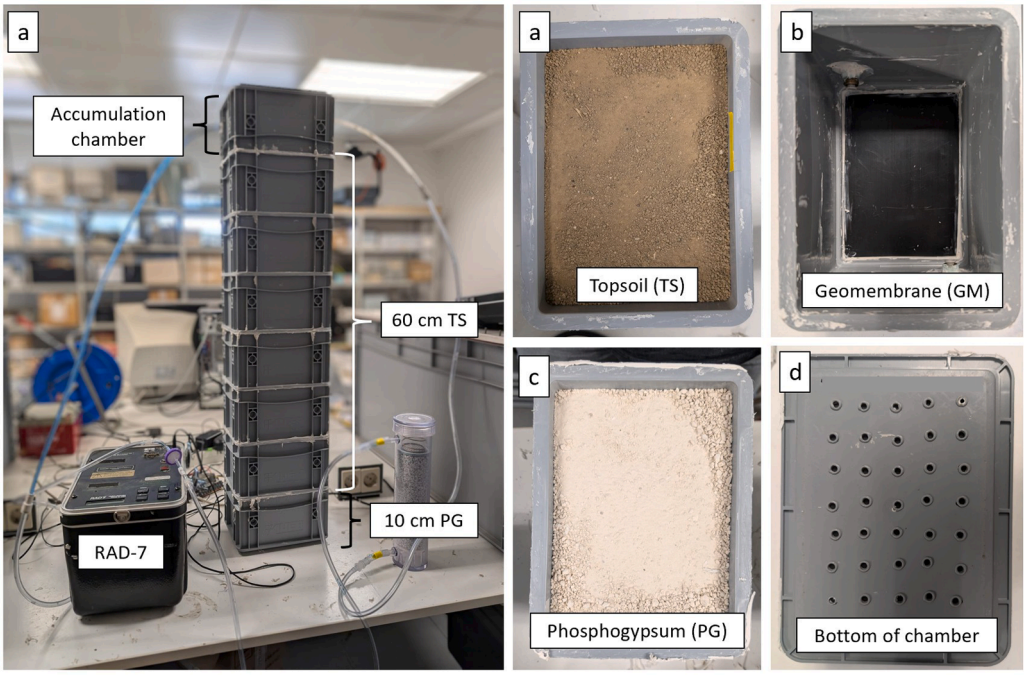

Fig. 2. a) Laboratory set-up and b-e) materials used for the measurement of the radon exhalation rate for the simulation of the Huelva phosphogypsum repository.

the results section.

$$-D\frac{dC(x)}{dx}|_{x=0} = 0 \tag{10}$$

The equation used for the radon diffusion coefficient is dependent on the porosity, water content of the soil and the medium temperature as follows [34]:

$$D(p,s) = D_0 p e^{-6sp-6s^{14p}} \tag{11}$$

- D_0: radon diffusion coefficient in air $(m^2\ s^{-1})$ [35]

$$D_0 = 1.1{\cdot}10^{-5}\left(\frac{T}{273}\right)^{\frac{3}{2}} \tag{12}$$

- T: medium temperature (K)

Finally, the calculation of the radon exhalation from the surface into the ambient, once the profile radon concentration in the material is known, is as follows:

$$E = -\beta D\frac{\mathrm{d}C(x)}{\mathrm{d}x}|_{x=d} \tag{13}$$

- E: radon exhalation rate $(Bqm^{-2}\ s^{-1})$

2.2. Algorithm

The algorithm used, RADEXH, is a modification of a previously developed code for the calculation of the radon diffusion coefficient, RADCO [36]. It solves the transport equation (Eq. 1) with the finite element method (FEM) in a one-dimensional mesh along the thickness of the soil with the standard Galerkin approach [37]. This will create a system of linear algebraic equations that will be solved using the standard Gaussian elimination method and the nodal concentration of the mesh will be given as a result. The size of the step was modified from 1 m to $1{\cdot}10^{-3}$ m to see which is a good compromise between a fast and accurate result by seeing how the solution converged to a value. The conclusion was that 0.01 m was the ideal step. The FEM discretization of Eq. 1 applied was described in Anex B of the supplementary material.

3. Methodology and materials

3.1. Methodology

3.1.1. Radon exhalation rate and emanation factor

There are different methodologies for the measurement of the radon exhalation rate and emanation factor [38–40]. The one chosen and applied in this study is based on letting the problem material exhale into an accumulation volume, which was developed in previous works [41–43]. The radon concentration in the volume over time has a known equation, which is a balance between the radon generated by the material and the radon that is lost by natural radon decay, the system leakage and the back-diffusion effect.

$$\frac{\mathrm{d}C(t)}{\mathrm{d}t} = \frac{ES}{V} - (\lambda_{Rn} + \lambda_b + \lambda_l)C(t) \tag{14}$$

- $C(t)$: radon concentration in the accumulation chamber (Bqm^{-3})
- t: time of the measurements (s)
- S: exhalation surface of the material (m^2)
- V: accumulation volume of the chamber (m^3)
- λ_b: bound exhalation constant (s^{-1})
- λ_l: leakage constant (s^{-1})

$$\lambda_{ef} = \lambda_{Rn} + \lambda_b + \lambda_l \tag{15}$$

- λ_{ef}: effective decay constant (s^{-1})

$$C(t) = C_{sat} + (C_0 - C_{sat})e^{-\lambda_{ef}t} \tag{16}$$

- C_0: initial radon concentration at the accumulation chamber (Bqm^{-3})
- C_{sat}: radon saturation concentration, that is $C(t{\to}\infty)$ (Bqm^{-3})

Different approximation can be done depending on the measuring time and the effective decay constant. By measuring the radon concen-

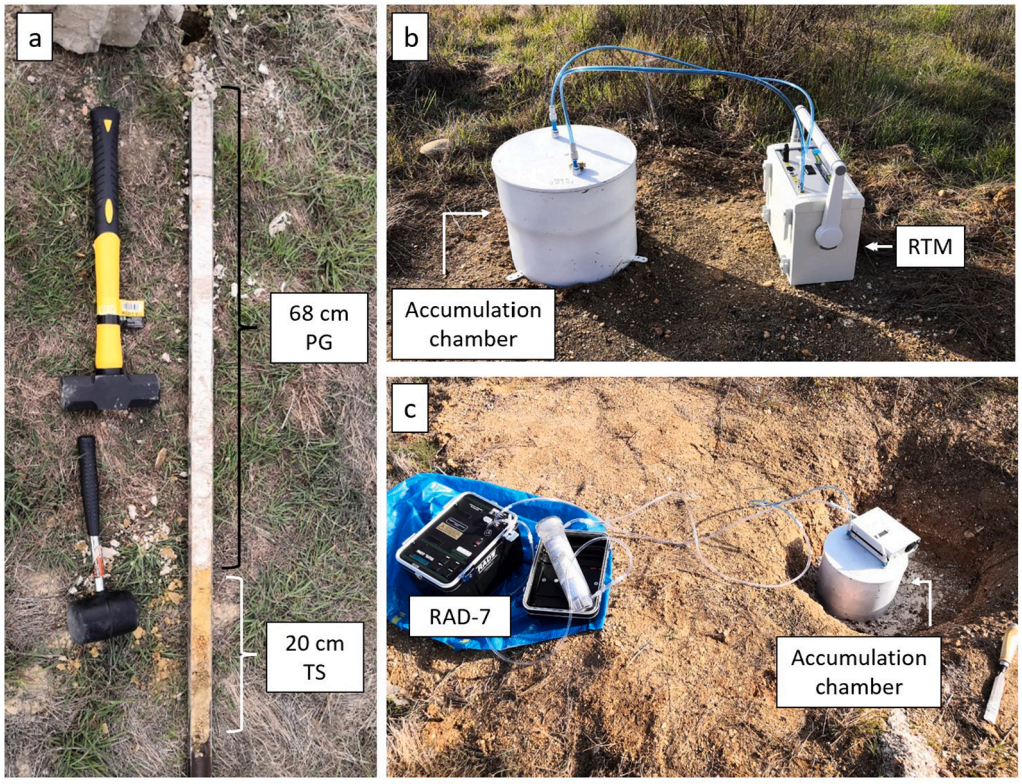

Fig. 3. a) Core sample taken and b-c) in-situ set-up for the measurements of the radon exhalation rate at the Huelva phosphogypsum repository. In c) the topsoil was eliminated to measure directly in the phosphogypsum.

tration in the volume of accumulation for an interval of time and fitting the data of radon concentration versus the measurement time using a known equation the radon exhalation rate and emanation factor can be calculated.

$$E = C_{sat}\lambda_{ef}\frac{V}{S} \tag{17}$$

$$\varepsilon = \frac{E}{S\lambda_{Rn}C_{Ra}^{226}m} \tag{18}$$

- m: mass of the sample (kg)

This methodology was applied both in a laboratory simulation of the repository and in-situ at the Huelva phosphogypsum repository.

3.1.2. Characterization of the materials

The porosity and real density of the phosphogypsum and topsoil samples was calculated using a pycnometer and calculating the apparent density using a probe of a known volume and weighing the sample in it. The samples were also weighed before and after drying them at 60ºC, until weigh was stable for a couple of days, and it was used to calculate the moisture content and relative humidity with Eqs. 5–6.

3.1.3. Radionuclides measurement

A coaxial HPGe extended range (XtRa)detector was used align with The Montecarlo Code LabSOCS [44,45] to determine the energy peak efficiency and the Genie 2000 [46] to apply the true coincidence summing corrections (TCS) using the Peak-To-Total method. The activity concentration of ^{226}Ra was determined both directly from the 186 keV photopeak and indirectly from the short half-life gamma-emitting progeny (^{214}Pb and ^{214}Bi). The interferences produced by ^{235}U in the 186 keV photopeak were removed by calculating the counts due to ^{235}U from the 63 keV photopeak of ^{234}Th [47,48]. Other radionuclides as ^{210}Pb, ^{228}Ra, ^{228}Th, and ^{40}K were also determined. The procedure for averaging samples, backgrounds and quality controls was accredited by ENAC based on the UNE-EN ISO/IEC 17025:2017 standard [49].

3.2. Laboratory experiments set-up

The materials used to emulate the phosphogypsum repository were: Phosphogypsum (PG), topsoil (TS), and a high-density polyethylene geomembrane (GM), as can be seen in Fig. 2. The combinations of the materials were the following:

- 0–0–10: 10 cm of PG.
- 0–30–10: 30 cm of TS + 10 cm of PG.
- 0–60–10: 60 cm of TS + 10 cm of PG.
- GM-0–10: 10 cm of PG + GM.
- 0–0–20: 20 cm of PG.
- 0–30–20: 30 cm of TS + 20 cm of PG.
- 0–60–20: 60 cm of TS + 20 cm of PG.
- GM-0–20: GM + 20 cm of PG.

The parameters used for the PG was a porosity of 0.5, a moisture content of 0.4, an emanation of 0.15, an activity concentration of ^{226}Ra of 669 Bq kg^{-1} and a bulk density of 1210 kg m^{-3}. For the TS the porosity was 0.4, the moisture content 0.2, the radon emanation rate 0.23, the activity concentration of ^{226}Ra 25 Bq kg^{-1} and the bulk density 1315 kg m^{-3}. The temperature was around 293.15 K and the ambient concentration was measured with the help of a Radon Scout (Sarad) and averaged a value of 10 Bq m^{-3}. After some testing a step in the mesh element of 0.01 m was chosen.

The radon monitors used for the measurements were one RAD7 (Durridge) and one RTM (Sarad). To avoid systematic differences in the measurements, the detectors were compared against each other using a reference soil [41]. Also, the RTM device was calibrated by SARAD with

Table 1
Radon transport models used on each of the references.

Case	Reference	Model type
1	[50]	1D steady state analytic solution
2	[25]	1D steady state analytic solution
3	[24]	1D steady state analytic solution
4	[24]	1D steady state analytic solution
5	[10]	3D transitory numerical solution with COMSOL
6	[10]	3D transitory numerical solution with COMSOL
7	[10]	3D transitory numerical solution with COMSOL
8	[27]	2D steady state numerical solution with RADON2D

date of 05/10/2023 and the RAD7 was calibrated comparing to the RTM. For this reason, both devices were used in the measurements without bias. The laboratory set-up (Fig. 2) consists of 2.4 L rectangular propylene chambers where the different materials will be placed and can be stacked on top of each other. Each of the pilled boxes were filled in a way that no air gaps were left between them. In total 6 kg of PG and 18 kg of TS were used (around 3 kg per chamber). An empty chamber with an entry and an exit for the connection with the radon detector is placed at the top to take measurements of the radon concentration and calculate the radon exhalation. The chambers are attached between them by using acrylic filler. Both the chamber material and the filler were tested to assure low radon leaks and verify its suitability.

3.3. In-situ measurements set-up

A similar concept is used for the in-situ set-up (Fig. 3). Two cylindrical propylene chambers of 9.7 L each, were placed on top of the repository in zone 1 to measure the radon concentration and obtain the radon exhalation. The measurements were done in zone 1, on top of the naked PG and on top of the topsoil cover. The chambers were inserted a few centimetres, one of them 3 cm and the other one 6 cm, to reduce the leaks and the strength of the back-diffusion effect [42]. Each chamber had an entry and an exit for the radon devices, the same as previously mentioned.

Additionally, a core sample was taken (Fig. 3) consisting of 68 cm of PG and 20 cm of TS. The core was divided into 13 section (3 of TS and 10 of PG), each measuring 6–8 cm. In these sections, the radionuclides were measured using gamma spectrometry, alongside the moisture content and relative humidity. More information about the core sections is displayed at Table SM1 in the supplementary material.

For RADEXH the parameters used for s and ^{226}Ra activity concentration are the one in Figs. 6–7 and Tables SM1-SM2. The porosity, radon emanation factor and the bulk density were 0.5, 0.15 and 1210 kg m^{-3} for the PG and 0.4, 0.23 and 1315 kg m^{-3} for the TS. The average temperature for the day and time of the measurements was 286.15 K and the radon ambient concentration was measured with the same Radon Scout monitoring the ambient concentration of the laboratory and had an averaged value of 22 Bq m^{-3}. The step in the mesh was 0.01 m.

4. Results

4.1. Validation

To validate the methodology, a comparison with the literature was carried out since there is no standard reference material for this measurement. The transport model used on each of the references can be seen in Table 1. The parameters given to the algorithm and taken from the respective references are presented in Table 2. Most cases are of homogeneous contaminated soil, except for cases 7 and 8. The first one is of a contaminated soil covered by a non-contaminated soil, and the second one is a stack of different contaminated soils.

Table 3 shows the algorithm results and the comparison with the ones given by the literature. In some cases of the literature, apart from calculating the radon exhalation using a model (Exhalation Reference in Table 3), they also took experimental measurements, in-situ or laboratory, (Exhalation Measurement in Table 3). Additionally, the relative difference (RD in Table 3) between our results and the references was calculated as $\mathrm{RD}(x,y) = \frac{y-x}{x}$.

As can be seen from the results, there is concordance between the predictions of our algorithm and the data in the literature, even reproducing the experimental results better than the model references for all cases except for case 4. On average, there is a 10% relative difference between our results and the experimental results, and a 14% relative difference between our results and the reference model results. The worst results are for the comparison with the reference model in case 2 and for the comparison with the experimental measurement in case 4. However, the similarity with the experimental measurement in case 2 is very good, with a relative error of only 3%. For case 4, our results are in

Table 3
Results of the exhalation for the different cases and comparison with the reference model result and experimental measurement, being RD the relative difference between the results that appear in the parenthesis, being RD the relative difference between the results that appear in the parenthesis.

Case	Exhalation (Bq m^{-2} s^{-1}) x10^{-2}			RD (Experimental, RADEXH) (%)	RD (Reference, RADEXH) (%)
	Experimental	Reference	RADEXH		
1	-	4.72	4.73	-	0.3
2	6.0 ± 0.6	4.7 ± 1.7	6.19	3	32
3	1.06	1.05	1.10	4	5
4	2.85	2.44	2.07	-27	-15
5	-	50.8	37.1	-	-27
6	-	22.6	19.1	-	-15
7	-	8.61	8.85	-	3
8	1.6 ± 0.3	1.77	1.50	-6	-15

Table 2
Input data from literature used for the validation of the methodology. p is porosity, s is moisture content, T is temperature, ε is radon emanation, $C_{Ra}^{226}$is the Ra^{226} activity concentration, ρ is the density, f is the radon generation rate, D is the radon diffusion coefficient, d is the thickness and C_{amb} is the ambient radon concentration.

Case	p	s	$T(K)$	ε	C_{Ra}^{226}(Bq kg^{-1})	ρ (kg m^{-3})	f (Bq m^{-3} s^{-1})	D (m^2 s^{-1}) x10^{-6}	d (m)	C_{amb} (Bq m^{-3})
1	0.3	0	-	-	-	-	0.129749	-	3	10000
2	0.37	0.064	293.15	0.22	59	1500	-	-	2	15
3	0.6	0.43	289	0.347	18	980	-	-	2	0
4	0.41	0.59	290	0.33	30	1570	-	-	2	0
5	0.5	0.1	283.15	0.2	500	1210	-	-	3	5
6	0.5	0.5	283.15	0.2	500	1210	-	-	3	5
7	0.5	0.5	298.15	0.2	500	1210	-	-	3	-
	0.5	0.6	298.15	0	0	-	-	-	0.4	5
8	0.3	-	-	-	-	-	0.041	1.3	0.3	-
	0.32	-	-	-	-	-	0.032	2.4	0.3	-
	0.32	-	-	-	-	-	0.032	2.5	0.4	-
	0.35	-	-	-	-	-	0.09	1.5	0.3	-
	0.43	-	-	-	-	-	0.075	1.2	0.2	0

Table 4
Input data used for the sensitivity analysis.

Parameter	Low	Medium	High
p	0.04	0.4	0.76
s	0.04	0.4	0.76
$T(K)$	275.15	293.15	311.15
ε_0	0.015	0.15	0.285
C_{Ra}^{226} (Bq kg^{-1})	35	350	665
ρ (kg m^{-3})	120	1200	2280
C_{amb} (Bq m^{-3})	1.5	15	28.5
d (m)	0.3	3	5.7

the same order of magnitude and the deviation from the reference model is only 15%. Therefore, when there is more discrepancy with one of the results, whether the experimental one or from reference model, the other one gives a lower relative difference. We can then conclude that we have successfully validated the algorithm through these comparisons.

4.2. Sensitivity analysis

We modified up to 8 parameters for the sensitivity analysis: the porosity, p, the fraction of moisture saturation, s, the medium temperature, T, the density, ρ, the activity concentration of ^{226}Ra, C_{Ra}^{226}, the radon emanation factor at dry conditions, ε_0, the ambient radon concentration, C_{amb}, and the thickness of the material, d. A low, medium and high values for each parameter were chosen, the middle one based in the usual values found in the literature and increasing and decreasing the parameter a 90% from its middle value. For the dry conditions emanation values was taken into account the use of Eq. 7, to not have invalid values, having for the emanation a minimum value of 0.03, for $s = 0.04$ and $\varepsilon_0 = 0.015$, and a maximum value of 0.81, for $s = 0.76$ and $\varepsilon_0 = 0.285$. The exhalation for every possible combination was computed, making 6561 cases. The values for the studied parameters are shown in Table 4.

With the data obtained for all combinations between the parameters in Table 4, the covariance between the exhalation and the input parameters was calculated along with the relative difference between the exhalation for the medium values of the input parameters (E_0) with the one obtained when increasing ($E_{+90\%}$) and decreasing ($E_{-90\%}$) each parameter and leaving the rest constant (Table 5).

We can see from the results that the most influential parameters are the ones that appear in the source equation (Eq. 2) and in the radon diffusion coefficient equation (Eq. 11), which are p, s, ε_0, C_{Ra} and ρ. This means that particular care should be taken when measuring them to ensure the lowest possible level of uncertainty. This is even more important for moisture content, as it is sensitive to ambient conditions. And finally, d, that does not appear directly in the equations, but it has some influence on the result. The one that influences less is the ambient concentration, C_{amb}, whose covariance factor is practically zero. The temperature is the one with the second lowest value as it influences in D thought D_0 (Eq. 12) and in E though β (Eq. 3), but the changes are not that significance in comparison with other parameter changes. Most of the parameters seem to be generally directly proportional except for s and C_{amb} which are inversely proportional. We can also see that the parameters always behave in the opposite way when increasing or decreasing. For example, when increasing s a 90% the exhalation will increase and when decreasing s a 90% the exhalation will decrease, being the relative difference positive and negative respectively. So, for each parameter we have a positive and a negative relative difference, except for p that the exhalation decreases in both cases.

The maximum and the minimum value obtain between all the 6561 cases are shown in Table 6 along with the input parameters for each case.

These results agree with the expected behaviour of the exhalation considering the equations. The parameters that appear in the source equation, ε_0, C_{Ra}^{226} and ρ, show a directly proportional relationship, so we find the minimum value of the exhalation for the values of $\varepsilon_0 = 0.015$, $C_{Ra}^{226} = 35$ Bq kg^{-1} and $\rho = 120$ kg m^{-3}, which are the lower values of these parameters and the maximum for the values of $\varepsilon_0 = 0.285$, $C_{Ra}^{226} = 665$ Bq kg^{-1} and $\rho = 2810$ kg m^{-3}, which are the highest values. The temperature also follows a directly proportional relationship, as β and D both increase when the temperature increases, from 275.15 K to 311.15 K, rising the exhalation as a result (Eq. 13). A higher β and a higher D means an easier transport thought the soil to the surface. As the ambient concentration influences the boundary condition (Eq. 9), its increase reduces the concentration gradient between the soil surface and the ambient and therefore the exhalation decreases. For the parameter d, a higher value of $d = 5.7$ m means there is more material to generate radon, resulting in a higher exhalation rate. The changes in p and s influence in the radon diffusion coefficient in a more complex way. What we can see with this result is that an increase in the moisture content translates to a lower exhalation, which makes sense physically as a higher water content will make the transport more difficult. In this case, for the porosity, we have the maximum exhalation for a value of $p = 0.76$ and the minimum exhalation for the value of $p = 0.04$, as with a higher porosity there will be more space for the radon to transport and in consequence a higher exhalation. This difference between the behaviour of p with the exhalation in Tables 5 and 6 could be for the change in moisture, as both if these parameters appear in the diffusion coefficient equation (Eq. 11). Figures showing the variation of the exhalation with each parameter, with curves for each combination, meaning in each curve the rest of the parameters are constant, was represented and can be seen in the supplementary material (Fig. SM2 to SM9). The previously explained behaviour of the parameters is observed in these figures as well.

Some of these parameters have a complex effect on radon exhalation. For example, the thickness of the exhalating material is critical when

Table 5
Result of the covariance between the 8 input parameters of the algorithm and the exhalation and relative difference between the exhalation for the medium values of the input parameters (E_0) with the one obtained when increasing ($E_{+90\%}$) and decreasing ($E_{-90\%}$) each parameter and leaving the rest constant.

	p	s	T	ε_0	C_{Ra}^{226}	ρ	C_{amb}	d
Covariance	0.207	-0.162	0.013	0.307	0.307	0.307	$-1.41 \cdot 10^{-5}$	0.147
$RD(E_0, E_{l-90\%})$ (%)	-92	6	-5	-90	-90	-90	$2 \cdot 10^{-3}$	-69
$RD(E_0, E_{+90\%})$ (%)	-9	-66	4	90	90	90	$-2 \cdot 10^{-3}$	0.3

Table 6
Maximum and minimum radon exhalation obtain for the in the sensibility analysis and the input parameters.

Exhalation (Bq m^2 s^{-1})	p	s	T (K)	ε_0	C_{Ra}^{226} (Bq kg^{-1})	ρ (kg m^{-3})	C_{amb} (Bq m^{-3})	$d(m)$
3.57	0.76	0.04	311.15	0.285	665	2280	1.5	5.7
$1.04 \cdot 10^{-5}$	0.04	0.76	275.15	0.015	35	120	28.5	0.3

Table 7
Input data for the analysis of p, s and d.

Case	p	s	T (K)	ε_0	C_{Ra}^{226} (Bg kg^{-1})	ρ (kg m^{-3})	C_{amb} (Bq m^{-3})	d(m)
1	[0.1,0.9] with 0.1 step	[0.1,0.9] with 0.1 step	293.15	0.15	350	1200	15	3
2	0.4	0.4	293.15	0.15	350	1200	15	[0.05,6] with 0.05 step

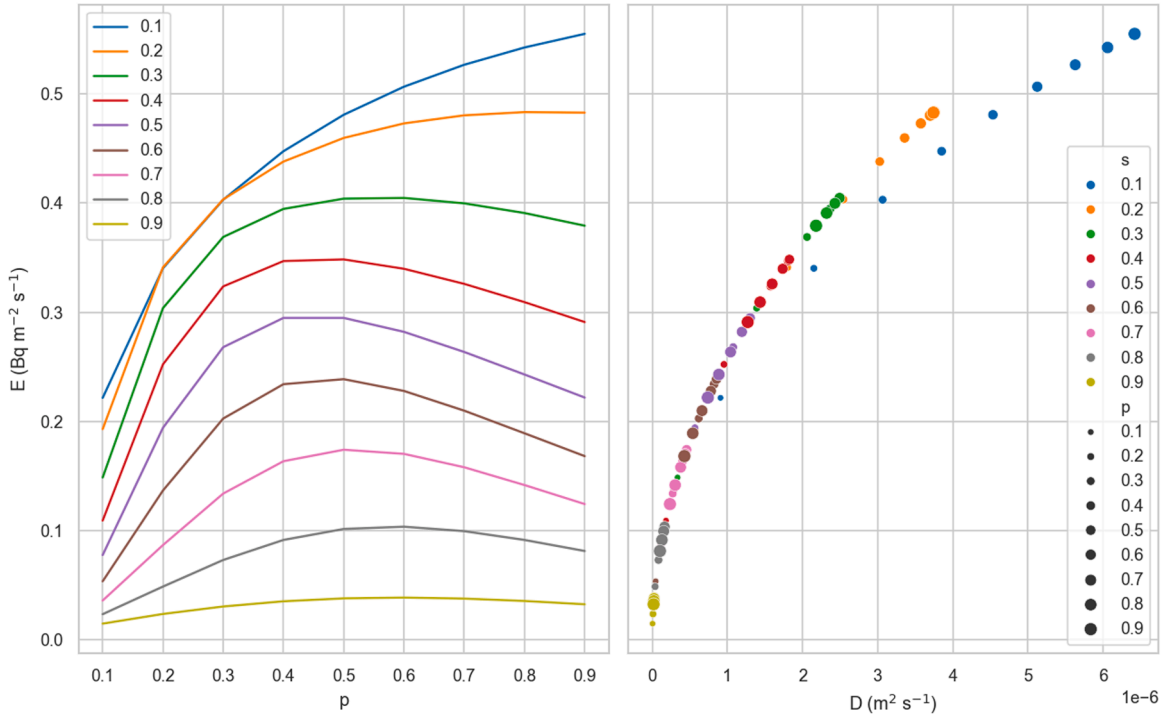

Fig. 4. Variation of the exhalation with a) porosity with different colour curves for different moisture contents and b) radon diffusion coefficient versus porosity (different marker size), and moisture (different colours). With the mean constant values of T = 293.15 K, d = 3 m, $\varepsilon_0 = 0.15$, $C_{Ra}^{226} = 350$ Bq kg^{-1}, $\rho = 1200$ kg m^{-3} and $C_{amb} = 15$ Bq m^{-3}.

considering the boundary conditions or the already mentioned effect of moisture content and porosity in the diffusion. Thus, a more detailed analysis of parameters *d*, *p* and *s* was done

For the case of the porosity, *p*, and the moisture content, *s*, a more detailed value sweep was done for a mean constant value of the rest of the parameters, in a range from 0.1 to 0.9 in steps of 0.1 for *p* and *s*, in all possible combinations. This was also done for the thickness of the material, *d*, for a constant value of the rest of the parameters, in a range from 0.05 m to 6 m in steps of 0.05 m. For this variation in *d* the two mentioned boundary conditions for the bottom of the soil (Eqs. 8 and 10) were tested. The values for these detailed cases are in Table 7.

Fig. 4 shows the results for case 1 in Table 7. In Fig. 4a we can see the radon exhalation as a function of the porosity with different curves for each of the moisture contents, and in Fig. 4b we can see the radon exhalation in function of the diffusion coefficient with different colours for the different moisture content and different point sizes for the different porosities.

As expected, the changes in the exhalation with *p* and *s* are directly related to the chosen diffusion coefficient equation (Eq. 9). In cases with a low moisture content, exhalation increases with higher porosity as there is more available space for radon transport, resulting in a higher diffusion coefficient and exhalation. This can clearly be seen in Fig. 4a in the blue ($s = 0.1$) and orange ($s = 0.2$) curve and at the end of Fig. 4b where the blue and orange points ($s = 0.1$ and $s = 0.2$) increase in size marker (in porosity) as the *D* increases.

As the moisture content rises, a higher porosity results in a lower diffusion coefficient and exhalation, as can be seen from the curves with $s \geq 0.3$ in Fig. 4a, and in the beginning and middle part of Fig. 4b where bigger markers of the same colour are lower in the curve than smaller ones. For example, for the green ($s = 0.3$) where the marker size for $p = 0.9$ correspond to a lower *D* than the marker sizes for $p = 0.8$–0.6. This is because a larger amount of water is stored at high porosities, which blocks a greater proportion of the small pores in the material and results in a lower diffusion coefficient and exhalation [51,52]. This proves that the algorithm is working correctly, as this is the expected behaviour from the used equation for *D*. Additionally, exhalation decreases with moisture content at the same porosities, but the effect of Eq. 7 can be seen in the slightly different trend for $s = 0.1$. For this value, the emanation is of 0.38, whereas for the other moisture values, the emanation is around 0.42, with variations of less than 1%. The emanation increases with moisture content as the water traps radon in the pores, preventing it from returning to the solid grains. This can be seen in Fig. 4a, which shows some overlap between $s = 0.1$ and $s = 0.2$, and in Fig. 4b, where the curve for $s = 0.1$ is displaced towards lower exhalations. However, it appears that the behaviour with *D* is more dominant.

Fig. 5 shows the results for case 2 in Table 7. In Fig. 5a the is a representation of the exhalation versus thickness (*d*), for different boundary conditions at the bottom of the soil. In Fig. 5b there is a graph of the contribution to the total exhalation, if the total thickness of a material was 6 m of ascending thickness and having the boundary condition at the bottom as flux null (Eq. 10). The contribution to the total was calculated as the division between the exhalation at the different thicknesses and the exhalation at a 6 m thickness, $\frac{E_{d=x}}{E_{d=6}}$.

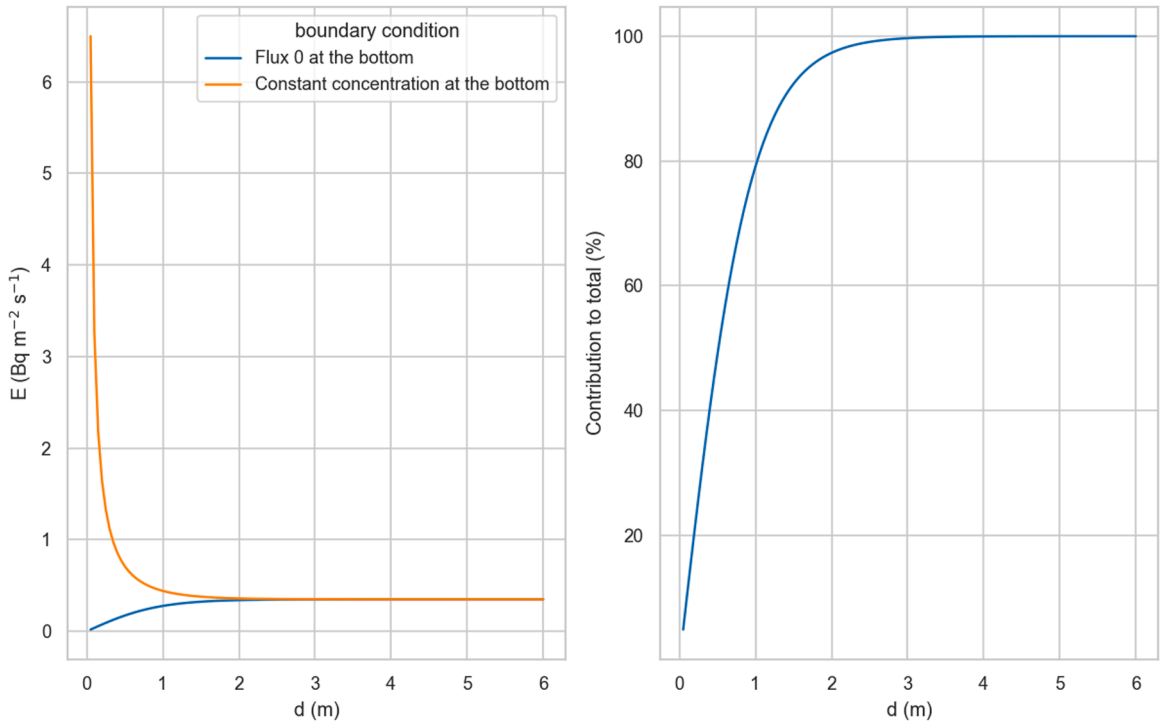

Fig. 5. a) Radon exhalation versus the thickness for two different boundary conditions at the bottom of the soil b) contribution of the different thickness to the final total exhalation of 6 m of soil having flux 0 at the bottom. With p = 0.4, s = 0.4, T = 293.15 K, $\varepsilon_0 = 0.15$, $C_{Ra}^{226} = 350$ Bq kg^{-1}, $\rho = 1200$ kg m^{-3} and $C_{amb} = 15$ Bq m^{-3}.

Table 8
Experimental and predicted result with the algorithm for the exhalation in the different set-ups of the prisms, along with the reduction of different covers, being RD the relative difference between the results that appear in the parenthesis.

Set-up	Exhalation (Bq m^{-2} s^{-1}) ·10^{-3}		RD (Experimental, RADEXH) (%)	Reduction (%)	
	Experimental	RADEXH		Experimental	RADEXH
0–0–10	18.1 ± 1.1	15.8	-12	-	-
0–30–10	9.7 ± 0.3	11	13	46	30
0–60–10	9.2 ± 0.6	10.3	12	49	35
GM-0–10	< 0.4	0.07	-	-	99.6
0–0–20	32.6 ± 0.4	31.7	-3	-	-
0–30–20	17.8 ± 0.6	21.7	22	45	32
0–60–20	16.4 ± 1.1	19.7	16	50	38
GM-0–20	< 0.2	0.07	-	-	99.78

With Fig. 5a we can see that Eq. 4 is not valid as a boundary condition for low thickness and once it reaches 1.5 the difference with the flux boundary (Eq. 10) is less than a 10%. This is important as Eq. 8 is a very used boundary condition sometimes for cases were the contaminated soil only reaches around 1 m where the relative difference between the conditions was around 30%. This discrepancy is due to the assumption done for boundary condition in Eq. 8 that the concentration at the bottom of the soil is equal to the concentration at a very large depth, when $x \to \infty$. So, the assumption that the thickness of the soil is deep enough to have that behaviour at the bottom of the soil happens only, or is a good approximation, from 1.5 onwards. This makes the null flux boundary condition a more appropriate one for wide range of thickness values. This is an important result, as this boundary condition is widely accepted in this type of problem. Although it is a good approximation that makes it easier to solve the transport equation, it is important to know its range of application.

Fig. 5b, shows that the first 50 cm is responsible of 50% of the total exhalation, while the 80% is provided by the top 90 cm of phospho-gypsum, reaching the saturation (99.9%) for around the top 3 m. This is consistent with the common practice of piling waste up in height rather than surface area reduces the exhalation rate.

4.3. *Laboratory experiments*

In Table 8 the exhalation value for the different configurations of the prism is shown for the experimental and simulated exhalation with our algorithm. The effective decay constant for these experiments varied around $5.1 \cdot 10^{-6}$-$1.21 \cdot 10^{-5}$ s^{-1} which are similar or close to the radon decay constant. The curve fit for of each exhalation result can be seen in Fig. SM10-SM15 in the supplementary material.

As we can see, the results agree with each other, although there are some differences. The mean relative difference between the predicted values and the experimental measurements is 13%, excluding the geo-membrane cases.

We can see that for the cases with the topsoil covers the algorithm prediction is higher than the experimental results. This may be because staking more chambers increases the experimental error by introducing small leaks in the experimental set-up and possible air gaps between chambers, even though the chambers are filled in order to prevent them, resulting in a non-continuous material profile unlike what the algorithm assumes. The pilling of the chambers also creates interfacial discontinuities where the chambers connect with each other which adds to the differences between the experimental set-up and the algorithm. Another

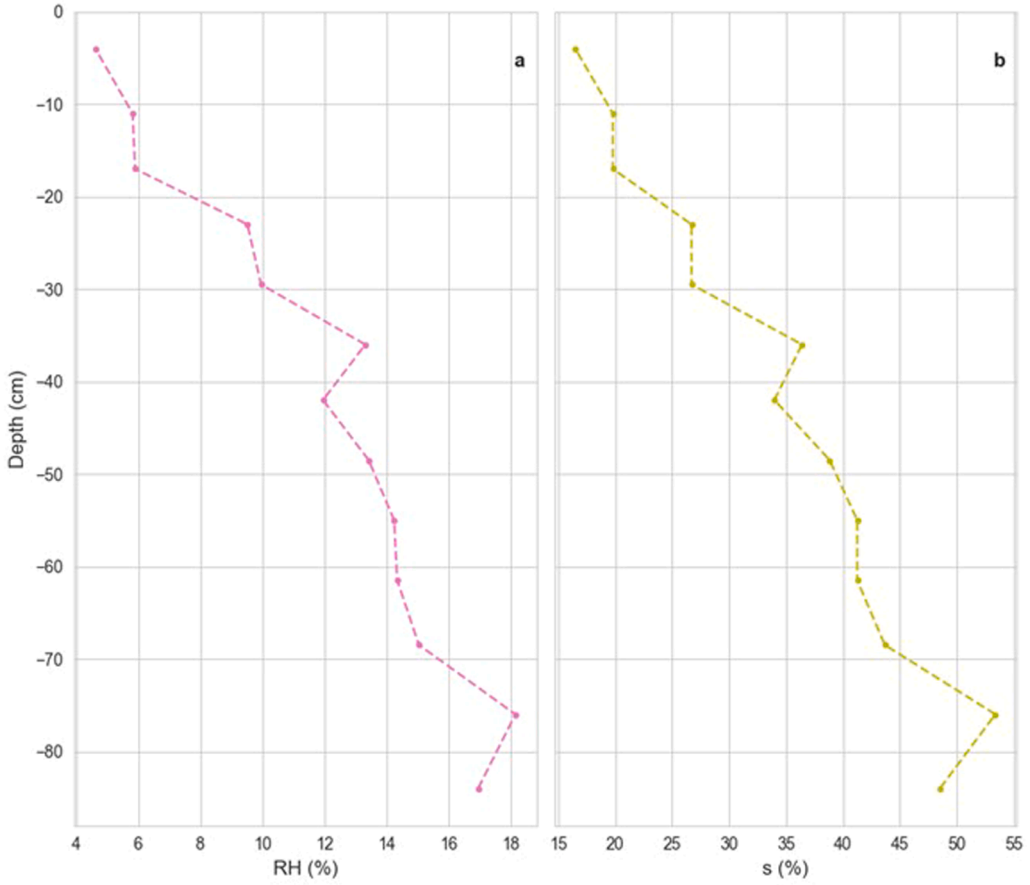

Fig. 6. a) Relative humidity content, RH, and b) moisture content, s, measured at different depths for the core taken in zone 1.

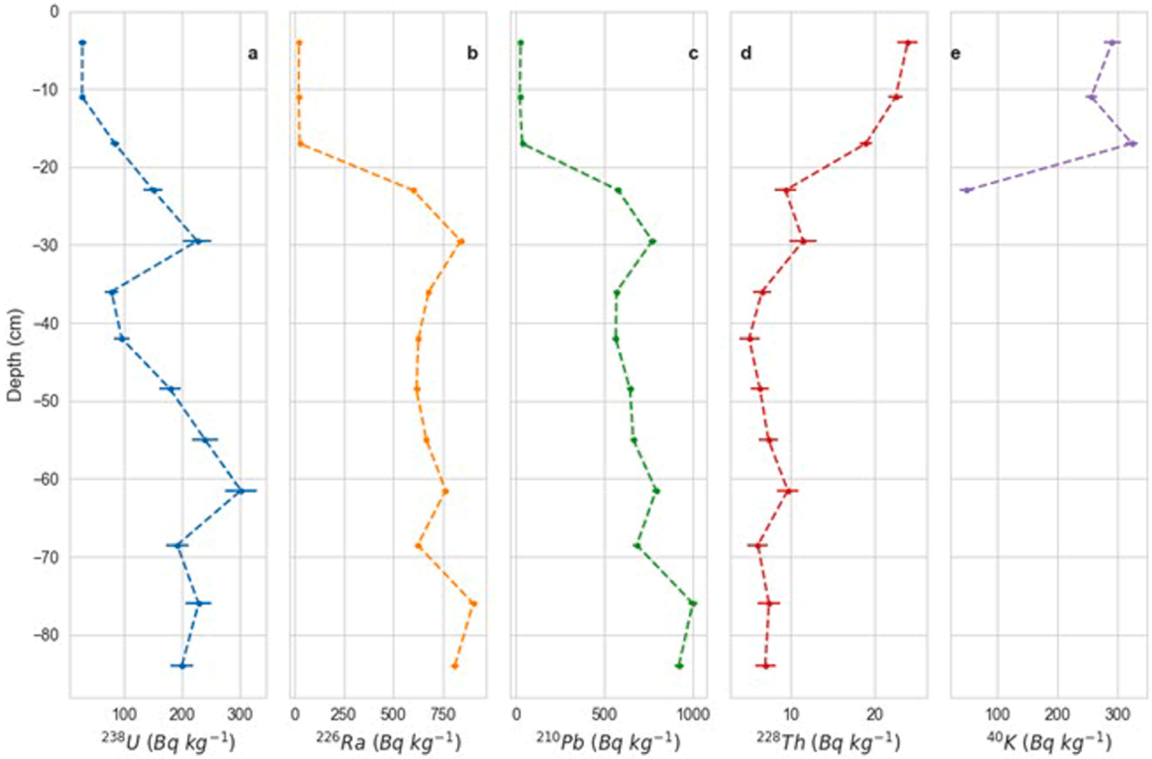

Fig. 7. Radionuclides, a) ^{238}U, b) ^{226}Ra, c) ^{210}Pb, d) ^{228}Th, f) ^{40}K, measurements at different depths for the core taken in zone 1. The points not represented in 40 K were below the detection limit of 48 Bq kg^{-1}.

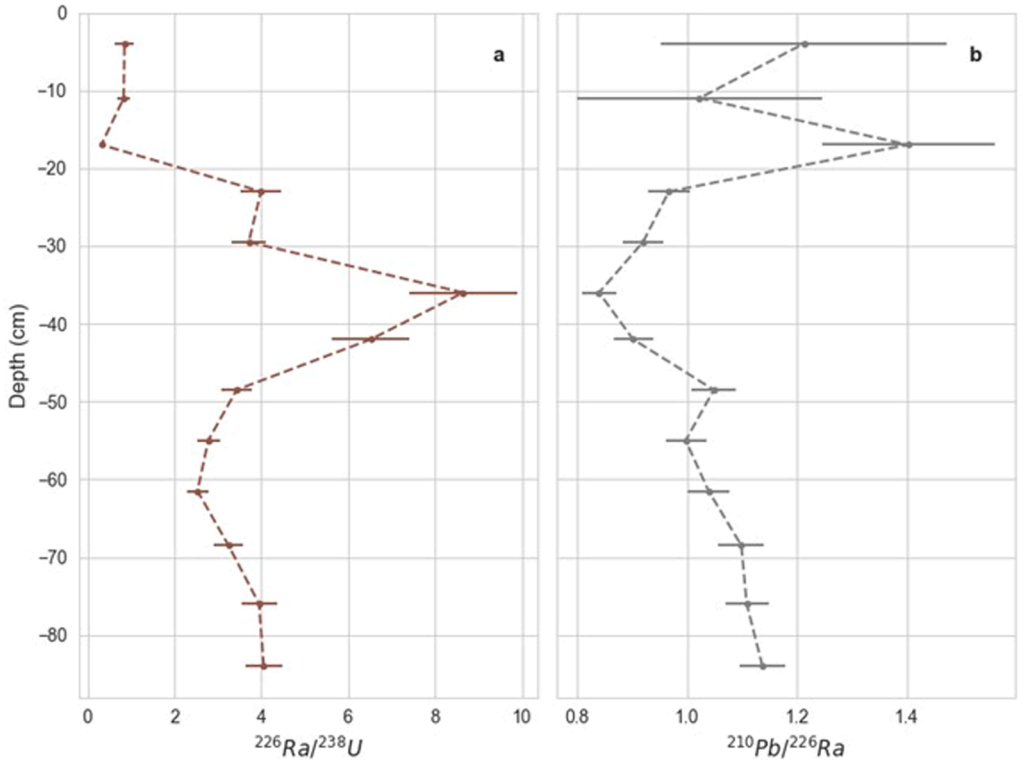

Fig. 8. Activity ratios, a) $^{226}Ra/^{238}U$, b) $^{210}Pb/^{226}Ra$, calculated at different depths for the core taken in zone 1.

possible source of error is the moisture content parameter. As explained in the previous section, this parameter is sensitive to changes and has a significant influence on exhalation. Even though precautions were taken and the measurements were carried out in a laboratory setting with no significant changes in humidity or temperature, the samples may have suffered small changes during the measurement period.

As expected, the GM cases had lower exhalation due to the low porosity and radon diffusion coefficient of high-density polyethylene materials, which makes it a common remediation solution. The exhalations for these GM cases were under the detection limit, making it the best cover against radon, and the results given by the algorithm agree with the limits. The radon diffusion coefficient used for the geomembrane was determined using the methodology explained in [36]. Also, pilling up PG increases the exhalation because, as we discussed in the previous section, most of the contribution to the exhalation in a porous material is given by the first meter and in our experimental conditions we only have 10 and 20 cm.

4.4. *In-situ experiments*

A core was taken from restored zone 1 of about 68 cm of PG and 20 cm of TS. The depth value in Figs. 6–8 are the mean point of the corresponding 13 sections of the core. The wet and dry masses were measured in different sections, and the relative humidity and moisture content were calculated from these measurements. (Table SM1 and Fig. 6).

As expected, the relative humidity (*RH*) is very correlated with moisture (*s*), finding a linear regression fitting of $r^2 = 0.98$, as both of them depend on the difference between the wet and the dry weight (Eqs. 4–6). The moisture content increases with the depth, ranging the relative humidity and moisture content for the topsoil of 5.4 and 15.7% and of 13.7 and 32.3% for the PG, respectively. There is a discontinuity in the interphase (from -17 cm to -23 cm), from -30 cm to -36 cm and from -69 cm to -76 cm, probably due to the hygroscopic properties of the PG for his P_2O_5 content, which makes it absorb surrounding moisture easily in combination with mixture in with the topsoil for the higher points. Also, the sample was taken in February after a period of 25 days without rains, which agrees with the data as there is humidity, but it does not reach very high values. The result for *s* at different points of the soil will be used as an input parameter for the algorithm.

The results for natural radionuclides concentrations are shown in Fig. 7, and the activity ratios of $^{226}Ra/^{238}U$ and $^{210}Pb/^{226}Ra$ in Fig. 8 are included (Table SM2). The ^{226}Ra values obtained were used as input for the algorithm.

For the topsoil the mean values obtained agree with previous measurements in that zone [8,9] and with non-perturbed soils from the world [53,54]. At the last topsoil point at -17 cm, the ^{238}U content is higher than for the other TS points, near to 100 Bq kg^{-1}, and a little bit for the ^{210}Pb, despite the ^{226}Ra content not being higher. This is ratified by the $^{226}Ra/^{238}U$ activity ratio at -17 cm (0.32 ± 0.03, so ^{238}U activity concentration is 3 times the ^{226}Ra one), meaning that there is no secular equilibrium between these radionuclides. The same but in a lower proportion happens for $^{210}Pb/^{226}Ra$, with a value of 1.40 ± 0.16 at -17 cm.

The mean activity concentrations measured for the phosphogypsum agree with the previously ones measured [8,9], with much high values for the ^{238}U, ^{226}Ra and ^{210}Pb in the PG than in the TS and the reverse for ^{228}Th and ^{40}K. In PG ^{40}K is around 10 times lower than in TS, although, a higher ^{40}K value is observed at PG1 compared to the other PG points. This could indicate a mixture of PG and TS in that section. For the activity ratios we can see that the ^{226}Ra and ^{232}U are not in secular equilibrium in the PG. The ^{210}Pb and ^{226}Ra are near to secular equilibrium for most of the points, with only a slightly disequilibrium for points -84 cm and -36 cm.

This disequilibrium between ^{226}Ra and ^{238}U in the PG and at point -17 cm could be due to the migration U from PG into TS due to the higher mobility of this radioelement in relation others as ^{226}Ra and ^{228}Th [55,56]. For the ^{210}Pb a similar effect can be seen, but in a much lower proportion.

The radon exhalation rate was predicted with our algorithm and

Table 9
Experimental and predicted result with the algorithm for the exhalation in the phosphogypsum repository, along with the reduction of the cover, being RD the relative difference between the results that appear in the parenthesis.

Set-up	Exhalation (Bq m^{-2} h^{-1})		RD (Experimental, RADEXH) (%)	Reduction (%)	
	Experimental	RADEXH		Experimental	RADEXH
PG	0.20 ± 0.13	0.19	6	-	-
PG + 20 cm TS	0.161 ± 0.004	0.15	5	18	17

measured experimentally. For these experiments, a period of measurement was chosen for which $\lambda_{ef}t \ll 1$, and a linear approximation to Eq. 16 was applied. In this approach the effective decay constant cannot be calculated. The results and comparison between them are shown in Table 9 and the curve fit of each exhalation result can be seen in Fig. SM16-SM17 in the supplementary material.

We can see that the simulated values are lower than the measured ones, with a relative difference of 6% with PG and of 5% with PG + 20 cm TS. This is a good result considering the approximations made in the algorithm. For example, it assumes a 1D mesh that does not consider possible lateral transport, a clean transition between the layers of the material, when, in reality, there is mixing at the interface between the PG and the TS, and a continuous material profile, as mentioned in the previous experiment. Another important difference is the possible discrepancy between the moisture in the in-situ setup and the moisture measured in the laboratory once the core was taken there as it is a sensitive and influential parameter. Also, the exhalation reduction for the 20 cm TS cover is similar for both results, of 18% for the experimental measurement and 17% for our algorithm. So, the mitigation evaluation is correct. The developed algorithm has the advantage that it can easily perform a sensitivity analysis, providing the conditions for the highest exhalation rate, so remediation can be planned considering possible variations from expected conditions.

5. Conclusions

The main conclusions were the following:

1. An algorithm to predict the radon exhalation rate of a multilayer porous material was developed and validated by comparing it with the literature and will be made available as an open-source software.
2. The sensitivity of the algorithm with the different input parameters was studied and it was found that the most influential ones are the source and diffusion parameters, that is, the emanation, density, ^{226}Ra content, porosity and moisture content.
3. A more detailed study was done for some of the most significance parameters (porosity, moisture content and thickness). In general, exhalation decreases with moisture content, but for some porosities at the lowest moisture value, the effect of moisture on the emanation creates a displacement to lower exhalations. For low moisture values, the radon exhalation rate increased with porosity, but for values higher than 0.3, there was a decrease in the exhalation rate with increasing porosity.
4. The fixed value boundary condition at the bottom of the material, a commonly used condition, was found to not give good results for material thicknesses lower than 1.5 m. This makes the null flux condition a more appropriate for a wider range of thickness values.
5. The first metre of material has the greatest influence on the final exhalation, of about 85% of the total contribution.
6. Given all this, the recommendation when using RADEXH is to pay special attention to measuring the emanation, density, ^{226}Ra content, porosity and moisture content, especially the latter as it is most sensitive to change. Using the flux null boundary condition is also recommended, as it provides a better representation of the experimental situation.
7. The Huelva phosphogypsum repository piles were simulated in the laboratory, and different cover materials were tested. A good agreement between the algorithm and the experimental results was found, with a mean relative difference of 13%. The cover material that achieved the highest exhalation reduction was a geomembrane sheet.
8. The experimental in-situ measurements in the phosphogypsum repository were done on top of the naked PG and on a topsoil cover. There was a relative difference of around 6% between our algorithm and the experimental result. The reduction of the topsoil cover was estimated correctly, with our algorithm showing a result of 16% and the experimental measurements of 17%.

To summarize, an open-source algorithm to predict the radon exhalation rate of a contaminated soil was developed and validated, and its dependence on different input parameters and boundary conditions was studied. It was then applied to the Huelva phosphogypsum repository, providing good results in the estimation of the radon exhalation rate and the reduction of different covers. Even though this model approximates the actual physical situation with a one-dimensional mesh steady-state diffusion transport model, the main novelty is its easy application to the specific problem of radon transport through a multilayer soil. Users only need to know the material's characteristics to estimate the radon exhalation rate, eliminating the need to adapt their problem to a broader software tool.

Environmental implication

The piling of waste materials is a common practice globally. If the repository contains naturally occurring materials waste with high 226Ra one of the main concerns is the radon that will be generated and exhaled into the environment. This makes the radon exhalation rate an important parameter to study when planning the restoration and mitigation. The main concerns are the workers in the area and the potential future use of the land, as continuous exposure to radon can lead to health problems. Therefore, the accessibility of a tool to predict the radon exhalation of a multi-layer material is of relevance.

CRediT authorship contribution statement

E. Castaño-Casco: Conceptualization, Investigation, Methodology, Software, Formal analysis, Data curation, Validation, Visualization, Writing – review & editing, Writing – original draft. **I. Gutiérrez-Álvarez:** Conceptualization, Investigation, Methodology, Resources, Software, Visualization, Writing – review & editing. **A. Barba-Lobo:** Conceptualization, Investigation, Writing – review & editing. **J.P. Bolívar:** Conceptualization, Methodology, Resources, Funding acquisition, Project administration, Supervision, Writing – review & editing.

Declaration of Competing Interest

The authors declare that they have no known competing financial interests or personal relationships that could have appeared to influence the work reported in this paper.

Acknowledgements

This research was partially funded by the Nuclear Safety Council (CSN) by the project “Radon exhalation from building materials;

Radiological impact and corrective measures (EXRADON)" (Ref.: PR-047–2021) and the project EPIT1432023 funded by the Regional Government of Andalusia.

Appendix A. Supporting information

Supplementary data associated with this article can be found in the online version at doi:10.1016/j.jhazmat.2026.141754.

Data availability

Data will be made available on request.

References

[1] Bolivar, J.P., Garcia-Tenorio, R., Garcia-Leon, M., 1995. Enhancement of natural radioactivity in soils and salt-marshes surrounding a non-nuclear industrial complex. Sci Total Environ 173 125–136.

[2] Mas, J.L., San Miguel, E.G., Bolívar, J.P., Vaca, F., Pérez-Moreno, J.P., 2006. An assay on the effect of preliminary restoration tasks applied to a large TENORM wastes disposal in the south-west of Spain. Sci Total Environ 364, 55–66. https://doi.org/10.1016/j.scitotenv.2005.11.006.

[3] Bolívar, J.P., Martín, J.E., García-Tenorio, R., Pérez-Moreno, J.P., Mas, J.L., 2009. Behaviour and fluxes of natural radionuclides in the production process of a phosphoric acid plant. Appl Radiat Isot 67, 345–356. https://doi.org/10.1016/j.apradiso.2008.10.012.

[4] Guimond R.J., Windham S.T., 1975. Technical Note ORP/CSD-75-3. Radioactivity distribution in phosphate products, by-products, effluents, and wastes.

[5] Santos, A.J.G., Mazzilli, B.P., Fávaro, D.I.T., Silva, P.S.C., 2006. Partitioning of radionuclides and trace elements in phosphogypsum and its source materials based on sequential extraction methods. J Environ Radio 87, 52–61. https://doi.org/10.1016/j.jenvrad.2005.10.008.

[6] Contreras, M., Pérez-López, R., Gázquez, M.J., Morales-Flórez, V., Santos, A., Esquivias, L., Bolívar, J.P., 2014. Fractionation and fluxes of metals and radionuclides during the recycling process of phosphogypsum wastes applied to mineral CO2 sequestration. Waste Manag 45, 412–419. https://doi.org/10.1016/j.wasman.2015.06.046.

[7] Bolívar, J.P., Garcla-Tenorlo, R., Garcia-León, M., 1996. On the fractionation of natural radioactivity in the production of phosphoric acid by the wet acid method. J Radio Nucl Chem Lett 214, 77–88.

[8] Dueñas, C., Liger, E., Cañete, S., Pérez, M., Bolívar, J.P., 2007. Exhalation of 222Rn from phosphogypsum piles located at the Southwest of Spain. J Environ Radio 95, 63–74. https://doi.org/10.1016/j.jenvrad.2007.01.012.

[9] Abril, J.M., García-Tenorio, R., Manjón, G., 2009. Extensive radioactive characterization of a phosphogypsum stack in SW Spain: 226Ra, 238U, 210Po concentrations and 222Rn exhalation rate. J Hazard Mater 164, 790–797. https://doi.org/10.1016/j.jhazmat.2008.08.078.

[10] López-Coto, I., Mas, J.L., Vargas, A., Bolívar, J.P., 2014. Studying radon exhalation rates variability from phosphogypsum piles in the SW of Spain. J Hazard Mater 280, 464–471. https://doi.org/10.1016/j.jhazmat.2014.07.025.

[11] Gatzweiler, R., Jahn, S., Neubert, G., Paul, M., 2001. Cover design for radioactive and AMD-producing mine waste in the Ronneburg area, Eastern Thuringia. Waste Manag.

[12] Harris, A.W., Atkinson, A., Claisse, P.A., 1992. Transport of gases in concrete barriers. Waste Manag 12, 155–178.

[13] EPA, 1979. A Preliminary Radiological Assessment of Radon Exhalation From Phosphate Gypsum Piles and Inactive Uranium Mill Tailing Piles.

[14] Hilal, M.A., El Afifi, E.M., Nayl, A.A., 2015. Investigation of some factors affecting on release of radon-222 from phosphogypsum waste associated with phosphate ore processing. J Environ Radio 145, 40–47. https://doi.org/10.1016/j.jenvrad.2015.03.030.

[15] Nisti, M.B., De Campos, M.P., Mazzilli, B.P., 2014. Natural radionuclides content and radon exhalation rate from Brazilian phosphogypsum piles. J Radio Nucl Chem 299, 261–264. https://doi.org/10.1007/s10967-013-2752-z.

[16] Lysandrou, M., Charalambides, A., Pashalidis, I., 2007. Radon emanation from phosphogypsum and related mineral samples in Cyprus. Radiat Meas 42, 1583–1585. https://doi.org/10.1016/j.radmeas.2007.04.006.

[17] UNSCEAR, 1988. Sources, Effects and Risks of Ionizing Radiation: United Nations Scientific Committee on the Effects of Atomic Radiation 1988 Report to the General Assembly, with annexes. United Nations.

[18] Dueñas C., Fernández M.C., Carretero J., Liger E., Pérez M., 1997. Release of 222 Rn from some soils. EGS-Springer-Verlag.

[19] Nazaroff, W.W., 1992. Radon transport from soil to air. Rev Geophys.

[20] Griffiths, A.D., Zahorowski, W., Element, A., Werczynski, S., 2010. A map of radon flux at the Australian land surface. Atmos Chem Phys 10, 8969–8982. https://doi.org/10.5194/acp-10-8969-2010.

[21] Antonopoulos-Domis, M., Xanthos, S., Clouvas, A., Alifrangis, D., 2002. Experimental and theoretical study of radon distribution in soil. Health Phys Soc.

[22] Maeng, S., Han, S.Y., Lee, S.H., 2019. Analysis of radon depth profile in soil air after a rainfall by using diffusion model. Nucl Eng Technol 51, 2013–2017. https://doi.org/10.1016/j.net.2019.06.018.

[23] Garcia Cadierno J.P., Suarez Mahou E., Matarranz J.L., Sainz C., Fernández Navarro P.L., Quindos L.S., 2005. Estimation of Indoor Radon-222 Concentration in Homes from Measurements of Natural Exposure Rates (The MARNA Project).

[24] Zhuo, W., Iida, T., Furukawa, M., 2006. Modeling Radon Flux Density from the Earth's Surface. J Nucl Sci Technol 43, 479–482. https://doi.org/10.1080/18811248.2006.9711127.

[25] Wu, J., Xie, R., Yi, H., Hu, T., Sun, J., Liu, Z., Li, H., liu, S., Yuan, S., Tan, Y., 2024. Laboratory study on the relationship between the vertical distribution of radon concentration in soil and the exhalation rate of radon from the soil surface. J Radio Nucl Chem. https://doi.org/10.1007/s10967-024-09755-5.

[26] Muñoz, E., Frutos, B., Olaya, M., Sánchez, J., 2017. A finite element model development for simulation of the impact of slab thickness, joints, and membranes on indoor radon concentration. J Environ Radio 177, 280–289. https://doi.org/10.1016/j.jenvrad.2017.07.006.

[27] Neznal M., Neznal M., Jiranek M., 2000. Comparison of Calculated and Measured Soil-gas Radon Concentration and Radon Exhalation Rate.

[28] Chitra, N., Sundar, S.B., Jose, M.T., Sivasubramanian, K., Venkatraman, B., 2019. A simple model to simulate the diffusion pattern of radon in different soil media. J Radio Nucl Chem 322, 1151–1158. https://doi.org/10.1007/s10967-019-06820-2.

[29] Porstendorfer J., Buttenveck G., Reineking A., 1994. Daily Variation of the Radon Concentration Indoors and Outdoors and the Influence of Meteorological Parameters.

[30] Sun, K., Guo, Q., Zhuo, W., 2004. Feasibility for mapping radon exhalation rate from soil in China. J Nucl Sci Technol 41, 86–90. https://doi.org/10.1080/18811248.2004.9715462.

[31] Clever, H.L., 1979. Solubility Data Series Krypton, Xenon and Radon - Gas Solubilities. Pergamon Press.

[32] Bilskie J., 2001. Soil Water Status: Content and Potential.

[33] IAEA, 2013. Measurement and Calculation of Radon Releases from NORM Residues. International Atomic Energy Agency.

[34] Rogers, V.C., Nielson, K.K., 1991. Correlations for predicting air permeabilities and " 'Rn diffusion coefficients of soils. Health Phys 61, 225–230.

[35] Schery S.D., Wasiolek M.A., 1998. Modeling Radon Flux from the Earth's Surface. pp 207–217.

[36] Castaño-Casco, E., Gutiérrez-Álvarez, I., Barba-Lobo, A., Bolívar, J.P., 2024. Development of a robust and precise methodology for the measurement of the radon diffusion coefficient in diverse materials. Constr Build Mater 440, 137402. https://doi.org/10.1016/j.conbuildmat.2024.137402.

[37] Taylor R.L., 2000. The Finite Element Method Fifth Edition Volume 1: The Basis.

[38] Pollet, L., Hult, M., Gryglewicz, G., D'Haen, J., Steensels, R., Schreurs, S., Schroeyers, W., 2025. Assessing the impact of phosphogypsum composition on radon exhalation from alkali-activated materials. J Hazard Mater Adv 20. https://doi.org/10.1016/j.hazadv.2025.100912.

[39] Kuzmanović, P., Todorović, N., Mrđa, D., Forkapić, S., Petrović, L.F., Miljević, B., Hansman, J., Knežević, J., 2021. The possibility of the phosphogypsum use in the production of brick: radiological and structural characterization. J Hazard Mater 413. https://doi.org/10.1016/j.jhazmat.2021.125343.

[40] Moreno, P., Noverques, A., Juste, B., Sancho, M., Verdú, G., 2024. Comparative analysis of techniques for estimating radon exhalation from building materials. Radiat Phys Chem 222. https://doi.org/10.1016/j.radphyschem.2024.111866.

[41] Gutiérrez-Álvarez, I., Martín, J.E., Adame, J.A., Grossi, C., Vargas, A., Bolívar, J.P., 2020. Applicability of the closed-circuit accumulation chamber technique to measure radon surface exhalation rate under laboratory conditions. Radiat Meas 133, 106284. https://doi.org/10.1016/j.radmeas.2020.106284.

[42] Gutiérrez-Álvarez, I., Guerrero, J.L., Martín, J.E., Adame, J.A., Bolívar, J.P., 2020. Influence of the accumulation chamber insertion depth to measure surface radon exhalation rates. J Hazard Mater 393. https://doi.org/10.1016/j.jhazmat.2020.122344.

[43] ISO, 2016. Measurement of Radioactivity in the Environment-Air: Radon-222-Test Methods for Exhalation Rate of Building Materials.

[44] Barba-Lobo, A., Expósito-Suárez, V.M., Suárez-Navarro, J.A., Bolívar, J.P., 2023. Robustness of LabSOCS calculating Ge detector efficiency for the measurement of radionuclides. Radiat Phys Chem 205. https://doi.org/10.1016/j.radphyschem.2022.110734.

[45] Suárez-Navarro, J.A., Moreno-Reyes, A.M., Gascó, C., Alonso, M.M., Puertas, F., 2020. Gamma spectrometry and LabSOCS-calculated efficiency in the radiological characterisation of quadrangular and cubic specimens of hardened portland cement paste. Radiat Phys Chem 171. https://doi.org/10.1016/j.radphyschem.2020.108709.

[46] Mirion Technologies, 2008. Coincidence Summing Library (Nuclides and lines). Canberra Industries, Inc., Meriden.

[47] Suárez-Navarro, J.A., Benavente, J.F., Expósito-Suárez, V.M., Caño, A., Hernaiz, G., Alonso, M.M., 2024. 226Ra activity concentration determined directly from the 186 keV photopeak using gamma spectrometry and a neural network. Radiat Phys Chem 217. https://doi.org/10.1016/j.radphyschem.2023.111486.

[48] Suárez-Navarro, J.A., Gascó, C., Alonso, M.M., Blanco-Varela, M.T., Lanzon, M., Puertas, F., 2018. Use of Genie 2000 and Excel VBA to correct for γ-ray interference in the determination of NORM building material activity concentrations. Appl Radiat Isot 142, 1–7. https://doi.org/10.1016/j.apradiso.2018.09.019.

[49] UNE IE, 2017. UNE-EN ISOIEC 170252017. General Requirements for the Competence of Testing and Calibration Laboratories.

[50] Andersen C.E., 1999. ERRICCA Radon Model Intercomparison Exercise. Riso National Laboratory.

[51] Hosoda, M., Shimo, M., Sugino, M., Furukawa, M., Fukushi, M., 2007. Effect of soil moisture content on radon and thoron exhalation. J Nucl Sci Technol 44, 664–672. https://doi.org/10.1080/18811248.2007.9711855.
[52] Zheng, X., Sun, Q., Liu, F., Deng, Y., Li, P., Huang, H., 2024. Effect of hygroscopicity of typical powder solid wastes on their radon exhalation characteristics. Sci Total Environ 944. https://doi.org/10.1016/j.scitotenv.2024.173956.
[53] UNSCEAR, 2000. Sources and Effects of Ionizing Radiation: United Nations Scientific Committee on the Effects of Atomic Radiation: UNSCEAR 2000 report to the General Assembly, with scientific annexes. United Nations.
[54] López I., Bolívar J.P., Fernández Caliani J.C., 2007. Niveles de radionucleidos en los suelos del norte de la provincia de Huelva e implicaciones dosimétricas. In: Bellinfante N, Jordán A (eds) Tendencias Actuales de la Ciencia del Suelo.
[55] Pérez-López, R., Álvarez-Valero, A.M., Nieto, J.M., 2007. Changes in mobility of toxic elements during the production of phosphoric acid in the fertilizer industry of Huelva (SW Spain) and environmental impact of phosphogypsum wastes. J Hazard Mater 148, 745–750. https://doi.org/10.1016/j.jhazmat.2007.06.068.
[56] Pérez-Moreno, S.M., Gázquez, M.J., Pérez-López, R., Vioque, I., Bolívar, J.P., 2018. Assessment of natural radionuclides mobility in a phosphogypsum disposal area. Chemosphere 211, 775–783. https://doi.org/10.1016/j.chemosphere.2018.07.193.